

Kinematically Lopsided Spiral Galaxies

R. A. Swaters, R. H. M. Schoenmakers, R. Sancisi and T. S. van Albada

Kapteyn Astronomical Institute, P.O. Box 800, 9700 AV Groningen, The Netherlands

ABSTRACT

Asymmetries in the distribution of light and neutral hydrogen are often observed in spiral galaxies. Here, attention is drawn to the presence of large-scale asymmetries in their kinematics. Two examples of kinematically lopsided galaxies are presented and discussed. The shape of the rotation curve –rising more steeply on one side of the galaxy than on the other– is the signature of the kinematic lopsidedness. It is shown that kinematic lopsidedness may be related to lopsidedness in the potential, and that even a mild perturbation in the latter can produce significant kinematical effects. Probably at least half of all spiral galaxies are lopsided.

Key words: galaxies: individual (DDO 9, NGC 4395); galaxies: kinematics and dynamics; galaxies: spiral; galaxies: structure

1 INTRODUCTION

Large scale asymmetries in the optical appearance of spiral galaxies have been known for a long time (e.g., M 101, Arp 1966), but only a few systematic studies have been carried out. Baldwin, Lynden-Bell & Sancisi (1980) drew attention to lopsided HI distributions of disc galaxies, emphasizing that the asymmetry affects large parts of the disc and that it is a common phenomenon among spiral galaxies. Also, they proposed a model in which the lopsidedness in a galaxy starts as a series of initially aligned elliptical orbits in an axisymmetric potential. Due to differential rotation, the pattern will wind up, however, and the lopsidedness will slowly disappear. They estimated that the typical lifetime of the lopsidedness is between 1 and 5 Gyr.

Richter & Sancisi (1994) made an estimate of the frequency of asymmetries from the shape of the HI line profiles. From an inspection of about 1700 global profiles they found that at least 50% of the galaxies have strong or mild asymmetries. This result has recently been confirmed by Haynes et al. (1998) who have obtained new, high precision global HI profiles for a sample of isolated spirals.

As both the disc kinematics and the HI density distribution determine the shape of the global profile, it is difficult to assess the nature of the asymmetry from the global profile alone. Richter & Sancisi (1994) emphasize, however, that the HI distributions and kinematics of individual galaxies indicate that the profile asymmetries often originate from a large-scale, structural lopsidedness affecting the whole disc, confirming the earlier findings of Baldwin et al. (1980).

In the mean time also the shape and brightness of the stellar discs have been investigated in a quantitative way. Rix & Zaritsky (1995) and Zaritsky & Rix (1997) found that about 30% of face-on field spirals show significant lopsidedness in the *I* and *K'* bands. Furthermore, galaxies with stronger lopsidedness have a *B*-band luminosity excess compared to the luminosity predicted by the Tully-Fisher relation. They suggest that the lopsidedness in the galaxies in

their sample is the result of recent accretion. Rix & Zaritsky (1995) derived a wind-up time of about 1 Gyr for their sample, contrasting the estimated lifetime based on their observed frequency of lopsidedness of about 3 Gyr. They also pointed out that the winding problem can be avoided if one assumes that the lopsidedness is caused by a lopsided potential, to which the gas and the stars merely respond.

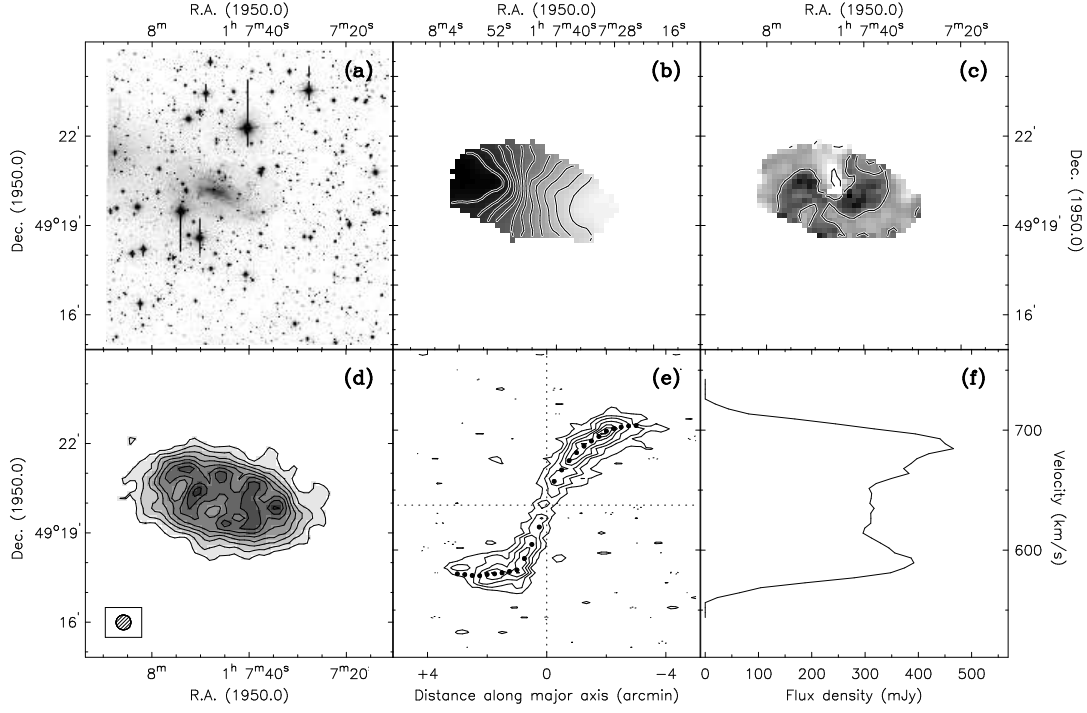
Aperture synthesis surveys of the HI distribution and kinematics of large numbers of spiral galaxies now provide abundant and sufficiently detailed information to investigate the nature of the asymmetries indicated by the global profiles. We have noticed that in a large number, perhaps the majority of cases, it is the kinematics rather than the HI distribution that determines the asymmetry in the global profiles. Galaxies with such asymmetric global profiles often have rotation curves that rise more slowly on one side of the galaxy than on the other. Correspondingly, the velocity field has isovelocity contours less curved on the side with the less steep rotation curve than on the other.

Here attention is drawn to the phenomenon of lopsided kinematics and two objects are shown to illustrate it. The HI observations are described and it is shown that a lopsided potential perturbation can produce the lopsided velocity fields. Finally, the question of the frequency of kinematically lopsided galaxies is addressed. It is worth noting that the two galaxies discussed here, as well as most of those identified as kinematically lopsided, are isolated systems and do not show signs of strong tidal interaction, nor is there clear evidence for ongoing accretion of satellite galaxies.

2 DATA AND ANALYSIS

Two objects, DDO 9 (UGC 731) and NGC 4395 (UGC 7524), have been selected here as representative examples of kinematically lopsided galaxies. Fig. 1 shows an overview of the data. The maps of the integrated HI emission, the position-velocity diagrams along the major axes and the global profiles originate from the Westerbork HI

DDO 9



NGC 4395

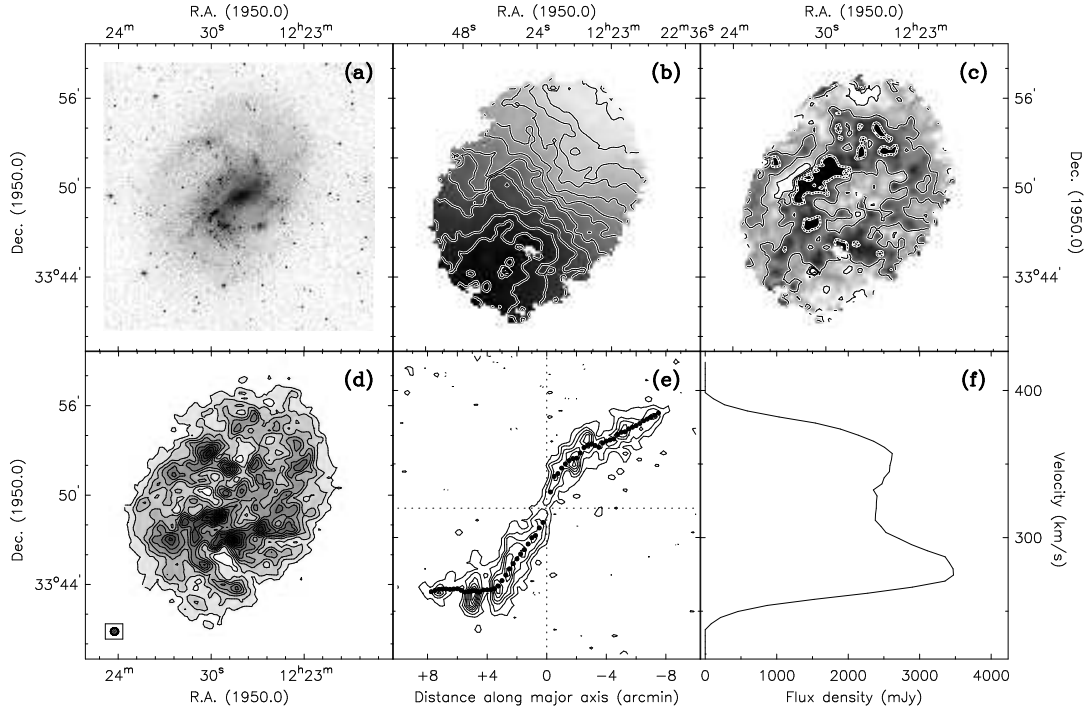


Figure 1. Data panels for DDO 9 and NGC 4395. (a) R-band image; (b) Velocity field from Gauss fits, dark shading indicates approaching side, contour levels are 590 to 690 km s^{-1} (DDO 9) and 260 to 380 km s^{-1} (NGC 4395), in steps of 10 km s^{-1} ; (c) Residual velocity field, dark shading indicates negative velocities, contours are spaced 7.5 km s^{-1} apart, negative contours are dotted; (d) Integrated HI map, the first contour level and the contour step are $2 \cdot 10^{20}$ HI atoms cm^{-2} , the hatched circle in the lower left shows the $30''$ beam; (e) Position-velocity diagram along the major axis, contours levels are -2σ , 2σ , 4σ , in steps of 2σ , $\sigma = 3.9$ mJy/beam for DDO 9 and 3.1 mJy/beam for NGC 4395, negative contours are dotted, the filled circles show the derived rotation curve; (f) Global line profile.

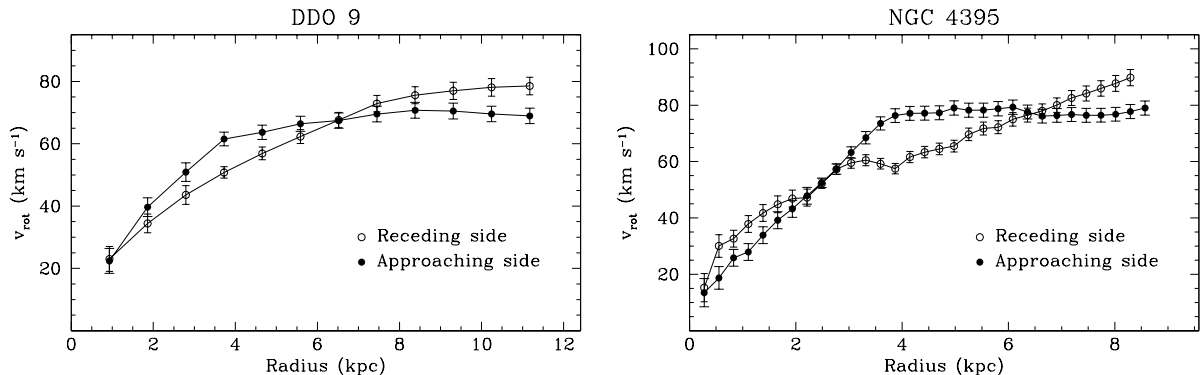


Figure 2. Rotation curves for the approaching and the receding sides separately. Open circles represent the receding side, filled circles the approaching side. The error bars are the formal errors in the fit, corrected for the beam size.

Survey of Spiral and Irregular Galaxies (WHISP, see Kamphuis, Sijbring & van Albada 1996), the optical *R*-band images are from Swaters & Balcells (1998).

The radial velocity fields shown in Fig. 1, panels *b*, were obtained from Gaussian curves fitted to the profiles. The rotation curve was derived by fitting tilted rings to the velocity field, using the method described by Begeman (1989). First, the kinematic centre was determined for all rings from a fit with all parameters free. In the case of NGC 4395, the average kinematic centre corresponded closely to the optical centre, and because of its higher precision, we used the latter. In the case of DDO 9, where the optical centre is not well determined, we used the centre that minimized the residual velocities, as is done in Schoenmakers, Franx & de Zeeuw (1997; hereafter SFdZ). By choosing the centre in this way, the difference between the rotation curves of the approaching and receding sides is minimized as well. SFdZ show that it is important to keep the centre fixed in these tilted ring fits, since a free centre will drift in such a way as to make a real $m = 2$ term disappear.

Another way of choosing the centre would have been to fix it in such a way that the outer parts of the rotation curves of the receding and approaching side coincide. This would mean that the gas in the outer parts moves on circular orbits and that all the asymmetry is concentrated in the inner parts. This would be a rather ad hoc choice, especially for NGC 4395. It demonstrates, however, that in a kinematically lopsided galaxy the centre cannot be determined uniquely from its kinematics alone.

Next, the systemic velocity was determined from a tilted ring fit with the centre fixed. The inclination and the position angle did not show systematic trends with radius, and hence they were fixed to their average values. Finally, with the parameters of each ring fixed as described above, the rotation curve was fitted with uniform spatial weighting to the velocity field as a whole, giving the average rotation curve. Rotation curves were also derived separately for the approaching and the receding sides in the same way. The latter are overplotted on the position-velocity diagrams in Fig. 1, panels *e*. A model velocity field was constructed from the average rotation curve, and subsequently subtracted from the observed one to give the residual velocity field shown in Fig. 1, panels *c*.

Both galaxies are lopsided in their kinematics. As can

Table 1. Properties of DDO 9 and NGC 4395.

	DDO 9	NGC 4395
Type	Im	Sm
Centre: $\alpha(1950)$	$1^h 7^m 46.7^s$	$12^h 23^m 19.9^s$
$\delta(1950)$	$49^\circ 20' 7''$	$33^\circ 49' 26''$
Systemic velocity (km/s)	638	320
Assumed distance (Mpc)	12.8	3.8
Absolute magnitude M_R	-16.9	-18.1
R_{25} (major \times minor, arcmin)	3.6×1.7	14.4×9.1
Inclination (degrees)	57	46
Position angle (degrees)	257	324
HI mass ($10^8 M_\odot$)	7.4	9.1

be seen in Fig. 2, the rotation curves for the approaching and the receding sides are distinctly different. In both galaxies, the rotation curve of the approaching side rises and subsequently flattens, whereas for the receding side it continues to rise. Obviously, the same pattern is seen in the position-velocity diagrams (Fig. 1, panels *e*). Accordingly, in the velocity fields the isovelocity contours are curved more strongly on the approaching side where the rotation curve becomes flat. This is best seen in NGC 4395. The residual velocity fields show clear systematic structure as well. In the case of DDO 9 a twofold structure is visible; NGC 4395 shows a more or less circular symmetric radial variation of the residual velocity, i.e., a radial variation of the systemic velocity. Note that the large-scale distributions of the HI and the stars are fairly symmetric, despite the lopsidedness in the kinematics.

To assist in the interpretation of the non-axisymmetric features of the motion of the gas, the velocity fields have been decomposed into harmonic components along individual rings, as found by the tilted ring fit, following the approach of SFdZ. As detailed results for several galaxies, including DDO 9 and NGC 4395, will be presented in a forthcoming paper (Schoenmakers & Swaters 1998), we restrict ourselves here to the main points. For both galaxies the dominant terms are $m = 0$ (circular symmetry), and $m = 2$ (bi-symmetry). DDO 9 has strong $m = 2$ terms, as expected from the twofold structure seen in the residual velocity field. The $m = 0$ term is weak. NGC 4395, on the other hand, shows a strong radial variation of the $m = 0$ term, and only weak $m = 2$ terms.

3 DISCUSSION

3.1 Kinematic lopsidedness versus lopsided potential

In Section 2 we showed that kinematically lopsided galaxies have velocity fields containing $m = 0$ and $m = 2$ terms. In the epicycle approximation, these harmonic terms in the velocity field can be related to potential perturbations. SFdZ showed that the line-of-sight velocity field contains $m - 1$ and $m + 1$ terms if the potential contains a perturbation of harmonic number m . Therefore, in the case of an $m = 1$ term in the potential (causing morphological lopsidedness), the line-of-sight velocity field will contain an $m = 0$ term and an $m = 2$ term, not necessarily with the same amplitudes. Hence, either or both of these terms should be visible in the residual velocity field. The relative strengths of these terms depend on the viewing angle of the perturbation ϕ_1 , as discussed below.

Expressions for the amplitudes of these harmonic components caused by an $m = 1$ perturbation in the potential are given by SFdZ in their equation A28. We have used the SFdZ relations to create a model velocity field. Using the axisymmetric part of the potential as derived from the mean rotation curve and a small, non-rotating ($\sim 10\%$) $m = 1$ perturbation, the corresponding line-of-sight velocity fields were calculated with different viewing angles. Fig. 3 shows the resulting velocity fields, projected with inclination $i = 55^\circ$, and viewing angle ranging from $\phi_1 = 0^\circ$ to $\phi_1 = 90^\circ$, in steps of 30° . A viewing angle of $\phi_1 = 0^\circ$ measured in the plane of the galaxy corresponds to a perturbation whose major axis is aligned with the observed minor axis of the system. For a viewing angle $\phi_1 = 90^\circ$, the velocity field shows the same characteristic asymmetry as seen in the observed velocity fields in Fig. 1. As the viewing angle decreases, the asymmetry becomes less pronounced. At the same time, the residuals change from being dominated by $m = 0$ terms for $\phi_1 = 90^\circ$ to $m = 2$ terms for $\phi_1 = 0^\circ$. For a viewing angle $\phi_1 = 0^\circ$, the rotation curves derived from the approaching and receding sides are identical, but the asymmetry between the approaching and the receding sides is replaced by a more subtle one between the near and the far side. Such an asymmetry would be difficult to find in observed velocity fields without a detailed harmonic analysis.

The dynamical basis of the models used to construct the velocity fields in Fig. 3 is weak. Therefore, no attempt has been made to reproduce the velocity fields of DDO 9 and NGC 4395 quantitatively. The models do illustrate, however, that a lopsided potential is capable of producing an asymmetric velocity field, and therefore an asymmetric rotation curve. The models do agree well with the observations qualitatively, i.e. they show strong curvature of the isovelocity contours on one side, corresponding to a relatively flat rotation curve, and nearly straight isovelocity contours on the other side, indicating solid body rotation. Furthermore, the models are useful in illustrating the effects of variations in the viewing angle.

The above analysis demonstrates that the cause of a lopsided velocity field can in principle be traced to a lopsided potential. It can be shown (Schoenmakers and Swaters 1998) that a 5-10% perturbation in the potential will give rise to an approximately 10-20% difference between the rotation curves of the approaching and receding sides. Hence, only a

mild perturbation of the potential is needed to produce a significant lopsidedness in the velocity field. Note that a small $m = 1$ potential perturbation will create morphological lopsidedness as well, also in the case of a non-selfgravitating component, since the orbits are no longer circular (e.g., Jog 1997).

3.2 Frequency of kinematically lopsided galaxies

There are many other galaxies showing the same kinematical pattern as the two objects described above. Striking examples are for instance UGC 5459 and NGC 2770 (Rhee and van Albada, 1996). The question now is: how common is kinematic lopsidedness among disc galaxies?

A first estimate of its frequency may be obtained from global profiles (Richter & Sancisi 1994, Haynes et al. 1998). This gives a fraction of $\sim 50\%$. However, global profiles are influenced by both the kinematics and HI distribution, as mentioned in the introduction. The effect of kinematic lopsidedness on the global profile can be seen clearly in Fig 1, panels *f*. Usually, on the side where the rotation curve becomes flat the corresponding horn in the global profile has a higher peak and is narrower, whereas on the side of the rising rotation curve it is wider and lower. NGC 4395 is a good example. However, since both the density distribution and the kinematics of the gas determine the shape of the global line profile, the two may conspire in such a way as to hide the expected signature. This is demonstrated in the case of DDO 9 (Fig. 1), where the flat rotation curve side produces the lower intensity horn. Furthermore, if the lopsidedness is oriented along the minor axis, it will not show up at all in the global profile. Inspection of the global profiles may, therefore, be helpful but is clearly insufficient for the purpose of recognizing the presence of kinematic lopsidedness.

On the basis of published HI maps and major axis position-velocity diagrams (Broeils & van Woerden 1994, Rhee & van Albada 1996), we estimate the fraction of kinematically lopsided galaxies to be roughly 15%. This fraction is a lower limit to the real fraction, because position-velocity diagrams along the major axis will miss lopsidedness directed along the minor axis. Similar estimates -at least 15%, but possibly up to 30%- are also obtained from the recent HI survey (Verheijen 1997) of a sample of about 40 spiral galaxies, which despite their membership of the Ursa Major cluster are believed to be representative for field galaxies. It should be noted that in all these selections by eye the fraction of lopsided galaxies will be underestimated because mild asymmetries, asymmetries observed under unfavourable viewing angles ϕ_1 , and asymmetries in nearly face-on galaxies will be missed. Therefore, the fraction of kinematically lopsided galaxies is probably at least 50%.

Kinematic lopsidedness need not always be the dominant perturbation in a galaxy. Schoenmakers (1998) studied the harmonic analyses of nine galaxies. Seven of these were taken from Begeman (1987), who selected large, regular, nearby spiral galaxies. The other two are LSB galaxies (van der Hulst, Zwaan & Bosma, priv. comm.). Out of these nine galaxies, seven show clear signs of kinematic lopsidedness in the harmonic decomposition, but only in three of these seven the lopsidedness is the dominant perturbation. In the other four the lopsidedness would not have been detected without harmonic analysis. It seems therefore that for

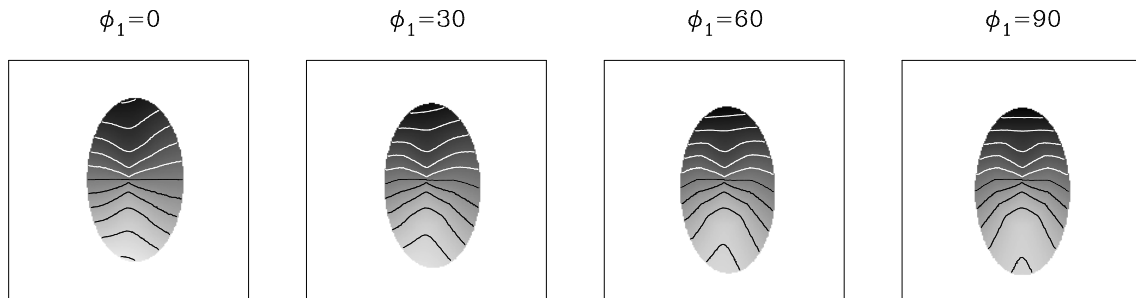


Figure 3. Model velocity fields derived from a lopsided potential. All fields have an inclination of 55° and a viewing angle ϕ_1 varying from 0° to 90° in steps of 30° , as indicated above each panel.

a reliable estimate of the frequency and distribution of amplitudes of kinematic lopsidedness it is necessary to examine the harmonic decompositions with care.

3.3 Origin of kinematic lopsidedness

We have found from HI observations that the kinematic lopsidedness has a well defined pattern that pervades the entire velocity field, and that it is a common phenomenon among apparently isolated galaxies. Optical (Rix and Zaritsky 1995, Zaritsky and Rix 1997) and infrared (Block et al. 1994) photometry shows that also the stellar discs are affected. These facts suggest that lopsidedness is structural to the disc, and that it is long-lived. Using epicycle theory, kinematic lopsidedness can be related to a lopsided potential. In the case of giant spirals the potential is probably governed by the disc, but in late type systems such as DDO 9 and NGC 4395 the halo contribution may well dominate. In such cases the lopsidedness may give information on the structure of the halo and the location of the visible galaxy inside it.

If the observed lopsidedness in galaxies is described as the result of a stationary lopsided potential perturbation the winding problem disappears, but the question arises of how to create and maintain such a potential. One possibility, of course, is a dynamical instability, e.g., of the type proposed by Sellwood & Merrit (1994). To create a strong $m = 1$ mode, their model requires strong counter-rotation. Though some galaxies are known to have counter-rotating gas or stars (e.g., Braun et al. 1994, Merrifield & Kuijken 1994), most galaxies do not (Kuijken, Fisher & Merrifield 1996). Sellwood & Valluri (1997) suggest that the dark halo could possibly be the counter-rotating component.

Lopsidedness may also be excited by interactions with a nearby neighbour or by accretion, as suggested by Odewahn (1996) and Zaritsky & Rix (1997) on the basis of optical observations. Since the galaxies presented here, and a large fraction of the galaxies inspected as described in section 3.2, do not appear to have companions, this would require that lopsidedness excited in this way must be a long lived phenomenon. Simulations do not rule out this possibility: Walker, Mihos & Hernquist (1996) have shown that accretion of a small companion by a large disc galaxy can create large scale asymmetries in the disc, that last up to about 1 Gyr. Furthermore, Weinberg (1994) has shown that

an $m = 1$ distortion in a King model is only weakly damped. In a halo-dominated galaxy, the passage or accretion of another galaxy could excite such an $m = 1$ perturbation in the halo that will persist for a long time (10-100 crossing times).

4 CONCLUSIONS

The presence of lopsidedness in the kinematics of disc galaxies has been established and the pattern recognized. Two examples from recent HI observations have been presented and discussed. A rotation curve which rises more steeply on one side of the galaxy than on the other is a clear signature of kinematic lopsidedness. A large fraction of spiral galaxies, probably at least 50%, is kinematically lopsided. Harmonic analyses of lopsided velocity fields show significant $m = 0$ and $m = 2$ terms. Using epicycle theory, kinematic lopsidedness can be related to a lopsided potential. A small $m = 1$ perturbation in the potential is sufficient to produce a significant lopsidedness in the velocity field.

The present study has revealed that the lopsidedness in the kinematics of spiral galaxies, as measured from the difference in rotation velocities between the approaching and receding sides, may reach amplitudes of order 10 – 20%. Larger kinematical disturbances have not been found among the galaxies examined and may not exist, except in case of strong tidal interactions. This seems to imply that perturbations in the potential of isolated disc systems, as proposed above as a mechanism to create kinematic lopsidedness, occur frequently but that their amplitudes are unlikely to exceed about 15%.

ACKNOWLEDGMENTS

The 21 cm line observations used in this paper are taken from the WHISP survey (Westerbork HI survey of spiral and irregular galaxies) carried out at the Kapteyn Astronomical Institute. The WSRT is operated by the Netherlands Foundation for Research in Astronomy with financial support from the Netherlands Organization for Scientific Research (NWO).

REFERENCES

Arp H., 1966, ApJS, 14, 1

- Baldwin J. E., Lynden-Bell D., Sancisi R., 1980, MNRAS, 193, 313
- Begeman K.G., 1987, PhD-thesis, University of Groningen
- Begeman K.G., 1989, A&A, 223, 47
- Block D. L., Bertin G., Stockton A., Grosbol P., Moorwood A. F. M., Peletier R. F., 1994, A&A, 288, 365
- Braun R., Walterbos R.A.M., Kennicutt R.C., Tacconi L.J.A., 1994, ApJ, 420, 558
- Broeils A., van Woerden, H., 1994, A&AS, 107, 129
- Haynes M. P., Hogg D. E., Maddalena R. J., Roberts M. S., van Zee L., 1998, AJ, 115, 62
- Jog C.J., 1997, ApJ, 488, 642
- Kamphuis J. J., Sijbring D., van Albada T. S., 1996, A&AS, 116, 15
- Kuijken K., Fisher D., Merrifield M.R., 1996, MNRAS 283, 543
- Merrifield M.R., Kuijken K., 1994, ApJ, 432, 575
- Odewahn, S., 1996, in Buta R., Crocker D.A. & Elmegreen B.R., eds, IAU Colloq. 157, Barred Galaxies, ASP Conf. Ser. 91, San Francisco, p. 30
- Rhee M.-H., van Albada T.S., 1996, A&AS, 115, 407
- Richter O.-G., Sancisi R., 1994, A&A, 290, L9
- Rix H.-W., Zaritsky D., 1995, ApJ, 447, 82
- Schoenmakers R. H. M., 1998, in preparation
- Schoenmakers R. H. M., Swaters R.A., 1998, in preparation
- Schoenmakers R. H. M., Franx M., de Zeeuw P.T., 1997, MNRAS, 292, 349 (SFdZ)
- Sellwood J. A., Merrit D., 1994, ApJ, 425, 530
- Sellwood J. A., Valluri M., 1997, MNRAS, 287, 124
- Swaters R. A., Balcells M., 1998, in preparation
- Verheijen M.A.W., 1997, PhD-thesis, University of Groningen
- Walker I. R., Mihos C., Hernquist L., 1996, ApJ, 460, 121
- Weinberg, M. D., 1994, ApJ, 421, 481
- Zaritsky, D., Rix, H.-W., 1997, ApJ, 477, 118